Available online at www.sciencedirect.com

ScienceDirect

Procedia Technology 26 (2016) 413 – 418

Procedia Technology

3rd International Conference on System-integrated Intelligence: New Challenges for Product and Production Engineering, SysInt 2016

Investigation on aging of metallic surface integrated micro-POFs

B. Hachicha[a,*], L. Overmeyer[a]

[a]*Leibniz Universitaet Hannover, Institute of Transport and Automation Technology, An der Universitaet 2, 30823 Garbsen, Germany*

Abstract

Surface integrated optical waveguides present a possibility to realize inherent communication structures. Optical communication is used particularly by smart parts exposed to humidity, high vibration or electromagnetic fields. We developed a method to integrate micro-polymer optical fibers (μ-POFs) into metallic surfaces using the dispensing process. After positioning, the μ-POFs are bonded to the surface by dispensing UV-curing adhesives. The bonded optical waveguide is coupled at its end-facets respectively to sender or receiver elements. Efficiency of the coupling depends on the alignment stability of the polymer fiber to beam sender or receiver. In operating conditions the smart parts undergo aging due to thermal and mechanical stress. We investigated the possible influence of this aging on the position stability of bonded μ-POFs, and consequently on the optical communication efficiency. The experimental set-up as well as the measurements are presented and discussed in this article.

Peer-review under responsibility of the organizing committee of SysInt 2016

Keywords: Optronic; optic; communication; surface inherent; System integration; aging;

1. Introduction

Integrated waveguides represent a current issue in scientific research. Innovative methods such as flexographic, inkjet printing [1] or hot-embossing [2] are investigated to realize polymer foil integrated communication and sensor systems [3]. Optical waveguides are also integrated into composite material [4] and civil buildings [5] for real time health monitoring. This offers the possibility of sensing forces [6], strain or temperature [7] and detecting damages [5]. Furthermore, the integration of waveguides into printed circuit boards (PCB) allows a high data transfer up to 15 Gb/s [8]. The optical waveguide's integration into PCB's is generally realized using photolithography, laser photo-pattering or direct dispensing methods [9].

However, exploiting this potential offered by integrated optical waveguides is not yet established for metallic and machine parts. To contribute to bridging of this gap, we are developing a method for flexible integration of micro-polymer optical fiber to metallic surfaces. A micro-dispensing process is used for this purpose in a 4-step process as presented and described in fig.1. The dispensed adhesive realizes the cladding of the core at the same time as bonding to the substrate surface.

* Corresponding author. Tel.: +0049-511-762-18321 ; fax: +0049-511-762-4007.
E-mail address: bechir.hachicha@ita.uni-hannover.de

Peer-review under responsibility of the organizing committee of SysInt 2016
doi:10.1016/j.protcy.2016.08.053

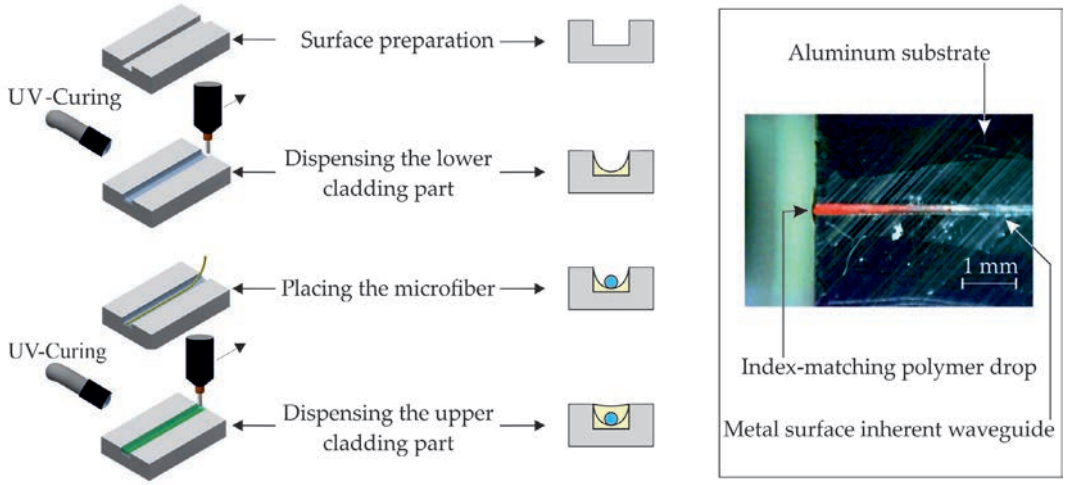

Fig. 1. **Process steps for surface integration of micro-polymer fibers**.In the first step a trench structure is created on the substrate surface along the desired path. In the second step the lower cladding layer is achieved by dispensing a UV-curing polymer adhesive along the path. In the third step the micro-fiber core is placed on the first cladding part. The fourth step is realized analogously to the first one and the upper cladding layer is dispensed.

The geometry of the lower cladding part defines essentially the height of the core in the trench. This position is considered for the alignment of optical axes between waveguide and beam sender or receiver while coupling. Alignment deviation decreases the coupling efficiency, thus the efficiency of the total optical communication path will decrease. In [10] we simulated as an example the height deviation limits for a coupling efficiency of 80%. This limit corresponds to $\pm$ 5 μm with a distance of $\approx$ 8.3 μm between beam sender and waveguide.
Under operating conditions the machine part undergoes mechanical as well as environmental stress. The question considered in this paper is the effect of this stress on the geometrical stability of the lower cladding part. The dependence of adhesive layer properties on aging effects is already known[11]. The chemical composition and the degree of cross-linking determine this dependence. Adhesives have a relatively inert chemical behavior, but nevertheless are able to interact with the surrounding atmosphere. The aging refers not only to possible subsequent changes in chemical and mechanical properties due to stress, moisture and temperature changes, but also to deformation due to fatigue in the polymer chains [11]. For this reason, we investigated the effect of such stress by practicing laboratory aging to a number of samples. The geometry of the cladding part is measured before and after undergoing the laboratory aging and the results are compared. In the following section methods and experimental procedures used in this context are presented. In the third section an interpretation of each experiment is provided. Finally, we discuss in the fourth section the results measured and pinpoint their meaning for the developed optical waveguides integration method.

2. Methods and experimental procedures

We prepared 16 samples (substrate: Al Mg4.5Mn0.7) with 4 trenches on each as shown in fig.2. One sample has the dimensions 40 x 10 x 8 mm^3. The trenches are 300 μm wide and 100 μm deep. We used the adhesive *Polytec UV2108* and dispensed the lower cladding layer using the precision-volume dosing unit *eco-PEN450* from *ViscoTec*. We adjusted the volume flow to 0.5 ml/min and the line dispensing velocity to 100 mm/s. Further details about the dispensing method adjustments are presented in [12].

We measured the topography of the trenches before and after dispensing the lower cladding layer. The measurements have been performed with a confocal microscope and a 20 times magnification objective lens (Nanofocus, μsurf custom system). After the samples preparation, we designed experiments for laboratory aging presented in tab.1. We considered 2 samples for every experiment (8 trenches). Furthermore, we realized a random distribution of the sam-

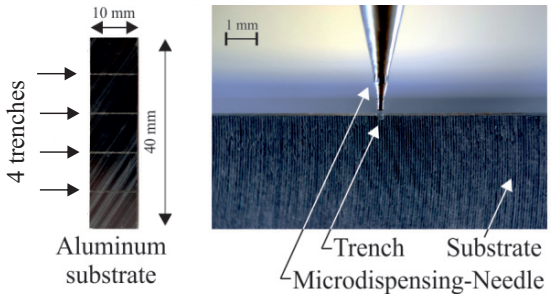

Fig. 2. **Example of a prepared sample for the presented experiences**. Samples are made from aluminum alloy Al Mg4.5 Mn 0.7. The surface is prepared with 4 trenches using micro-milling process. One trench is $300 \pm 29.90\mu m$ wide and $100 \pm 15\mu m$ deep. The lower cladding layer is dispensed using a precision-volume dosing unit and a micro-dispensing needle.

ples to the experiments in order to compensate possible stochastic influences during preparation.
Three laboratory aging processes were considered. The first one was based on the guide to the selection of standard laboratory aging conditions for testing bonded joints (ISO 9142:2003). During this laboratory aging, the sample was subjected to temperature and humidity changes in a climate chamber during 2 cycles of 12 hours. In one cycle the temperature is increased to $70°C$ and the relative humidity to 90% during 6 hours. Then the temperature is decreased to $-40°C$ during 5.5 hours. Finally the climate in the chamber is changed to $24°C$ and 50% relative humidity for the last 30 minutes.
The second laboratory aging process was a dynamic stress applied to the samples. In a joint project, the waveguide will be integrated on the surface of a sensory axis slide for machine tools [13]. In this axis a maximal strain of $10^{-6}\ m/m$ was measured. We considered a coefficient of safety totaling 2.5. This leads to a strain of $10^{-6}\ m$ by a sample length of 40 mm. Correspondingly, we applied 6000 sinusoidal tension-compression stress cycles to the samples with a frequency of 10 Hz using a hydropulser.
The third aging process was based on the methods of exposure to laboratory light sources (UV-Lamps) presented in the standard ISO/FDIS 48923:2015. We applied the B-method with an equivalent intensity to 0.76 $W/(m^2 \cdot nm)$ during 24 hours. We used for this purpose the *panasonic* UV-control device *UJ35* with the lamp *ANUJ6184* and a 3 mm spot diameter at a 385 nm wavelength. After every experiment presented in tab.1, the topography was measured using confocal microscopy. The results of these measurements are presented in the following section.

Table 1. **Design of experiments for laboratory aging.** The + sign means that the sample was subjected to the mentioned aging process. The - sign means that the sample was not subjected to the mentioned aging process.

Exp.	Samples		Climatic chamber	Dynamic stress	UV-Radiaiton
1	12	13	+	+	+
2	5	2	+	+	-
3	7	15	+	-	+
4	4	14	+	-	-
5	3	8	-	+	+
6	9	11	-	+	-
7	6	16	-	-	+
8	1	10	-	-	-

3. Results

The geometry of the lower cladding layer is relevant for the core height inside the waveguide. The position of the core is relevant to realize coupling to a sender or receiver element. The stability of efficiency for a realized coupling depends on the stability of the core position. To investigate whether aging has any influence on the geometry of the

first cladding part and therefore on the position stability of the optical core, we scanned the topography of the lower cladding using confocal microscopy before and after performing laboratory aging. In fig.3 the mean trench depth is shown as well as the mean height of the lower cladding for the prepared 64 trenches. The thickness of the lower cladding varies between 7.6 μmm and 43.5 μmm (Fig.3).The standard deviation of measured first cladding layers is 9.51 μm. In [10] we determined a height position variation of about ± 5 μm to be relevant for a distance of ≈ 8.3 μm between Sender and optical waveguide. Using this information and the statistical confidence interval calculation [14], at least 54 trenches have to be examined. Thus, the 64 realized trenches ensure statistical relevance.

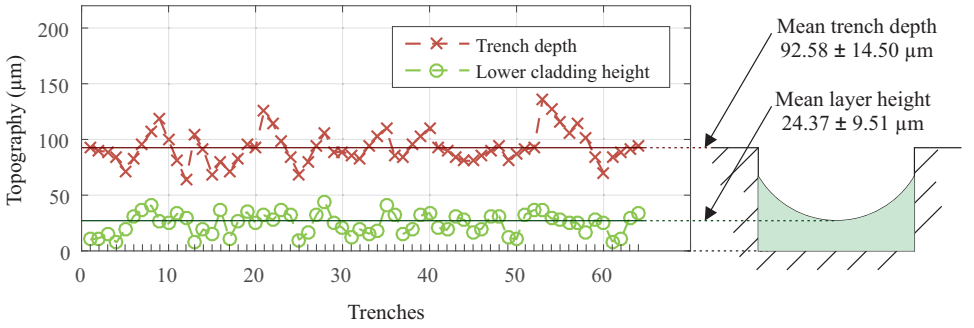

Fig. 3. **Average depth of 64 prepared trenchs and the average height of the dispensed lower cladding**. 16 substrate samples (40 mm x 10 mm x 6 mm) were prepared with 4 trenches on each. The depth of the empty trench (crosses) as well as the height of the dispensed lower cladding (circles) inside the trench was determined using confocal microscopy as described in sec.2.

We selected 6 samples and exposed every group of two (8 trenches) to one of the aging tests presented in section 2. Fig.4 shows the measured lower cladding height after these tests. The most significant difference is observed by the 2nd, 3rd and 4th trench of sample 11 (dynamic stress) as well as the 2nd trench of sample 6 (UV radiation). The measured height differences here are between 7.1 μm and 9.8 μm. However, the effect has no significance if we realize an evaluation based on statistical confidence interval calculation [14].

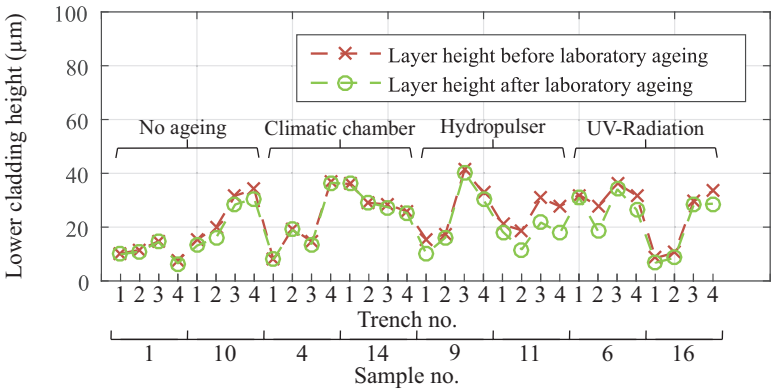

Fig. 4. **Measured height of the lower cladding after exposing samples to laboratory aging**. The first group of two samples (8 trenches) was exposed to no aging, the second group to humidity and temperature cycles, the third group to dynamic stress and the fourth group to to UV-exposure (sec.2). The height values of the lower cladding before (crosses) and after aging (circles) are measured using confocal microscopy (sec.2).

We want to ensure that a combination of the aging tests does not lead to different effects on the lower cladding height. Accordingly, we created for this purpose 4 groups of 2 samples each. 3 groups were exposed subsequently to two different aging tests. The fourth group was exposed to all 3 aging tests in a row as shown in fig.5. The height

values of lower cladding show no significant difference to the values in fig.4 as well as to the measured height before aging. To confirm the observed combination effects, we evaluated the results based on statistical confidence interval calculation [14]. The effect of a combination of different methods has no significance on the measured lower cladding height.

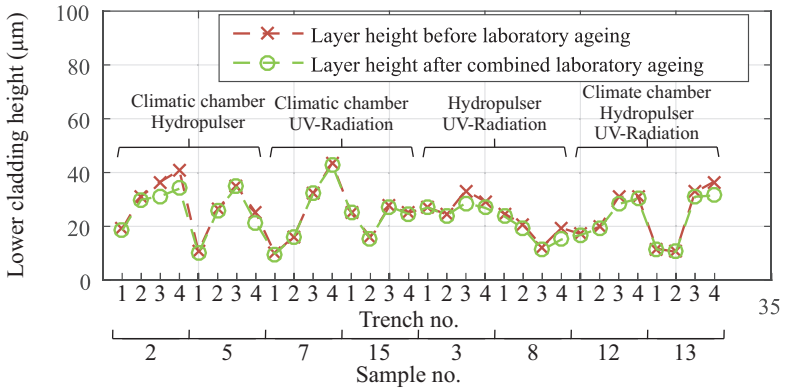

Fig. 5. **Measured height of the lower cladding after exposing samples to combined laboratory aging**. The first three groups of two samples (8 trenches) were exposed to two aging methods. The fourth group was exposed to all aging methods presented in sec.2. The height values of the lower cladding before (crosses) and after aging (circles) are measured using confocal microscopy (sec.2).

In summary, we showed here that aging of the lower cladding has no significant effect on the stability of its height. The selected adhesive for the presented optical waveguide surface integration method is suitable for the operation conditions.

4. Discussion

Offsets between the optical axis of an optical waveguide and sender or receiver are know to decrease the coupling efficiency[15]. Adhesives are typically used for joints to fix the position of waveguide and sender after the alignment of their optical axis. However, the exact geometrical change due to adhesive aging is generally not known. This change depends on the chemical composition of the adhesive as well as the degree of cross-linking with the bonding partner. In case of surface integrated micro-POFs, *Polytec UV2108* adhesive is used for cladding and for bonding to the substrate surface. The height of the lower cladding directly influences the core position. We show in this paper that laboratory aging does not lead to significant changes in cladding height. Combination of different aging processes as well does not affect the lower cladding height. The UV-adhesive *Polytec UV2108* is adequate to bond the waveguide without position deviation due to aging effects. We demonstrated form stability of cladding layers realized with the UV-adhesive *Polytec UV2108* and their resistance to laboratory aging methods. However, aging can also have an effect on optical properties and the adhesion between substrate and cladding as well as between cladding and core material. For this purpose, we are planing in near future to investigate this point.
Moreover, we can observe a 14.5 μm standard deviation in the measured trench depth and 9.51 μm in the measured lower cladding height. These deviations affect the repeat accuracy of the presented optical waveguide integration method. To increase accuracy, the trench geometry has to be measured in advance. Depth deviations have to be considered to actively regulate the dispensing process. Dispensing a defined and controlled volume along the trench depending on the measured local depth deviation can ensure a stable lower cladding height. We are investigating the use of a confocal sensor for this purpose and the results will be presented in a future publication.

Acknowledgments

This research project is part of the Collaborative Research Centre program SFB 653 - Gentelligent Components in their Lifecycle - Utilization of Inherent Information in Production Engineering (www.sfb653.unihannover.de). The authors want to thank the German Research Foundation (DFG) for supporting and funding this research project.

References

[1] Wolfer, T., Bollgruen, P., Mager, D., Overmeyer, L., Korvink, J.G.. Flexographic and inkjet printing of polymer optical waveguides for fully integrated sensor systems. Procedia Technology 2014;15:521–529. doi:10.1016/j.protcy.2014.09.012.

[2] Rezem, M., Günther, A., Rahlves, M., Roth, B., Reithmeier, E.. Hot embossing of polymer optical waveguides for sensing applications. Procedia Technology 2014;15:514–520. doi:10.1016/j.protcy.2014.09.011.

[3] Wolfer, T., Bollgruen, P., Mager, D., Overmeyer, L., Korvink, J.G.. Printing and preparation of integrated optical waveguides for optronic sensor networks. Mechatronics 2015;doi:10.1016/j.mechatronics.2015.05.004.

[4] Basile, E., Brotzu, A., Felli, F., Lupi, C., Saviano, G., Vendittozzi, C., et al. New magnetic connector for embedding of optical sensors in composite materials. In: Brotzu, A., Felli, F., Lupi, C., Saviano, G., Vendittozzi, C., Caponero, M.A., editors. New magnetic connector for embedding of optical sensors in composite materials. 2011, p. 521–526. doi:10.1109/ICSensT.2011.6137034.

[5] Yan Qixiang, , Coll. of Civil Eng., Southwest JiaoTong Univ., Chengdu, China, , Cheng Xi, , Ding Rui, , editors. Application of distributed optical technique in sensing interface disengaging and cracks of steel tube-confined concrete. 2011.

[6] Park, Y., Ryu, S., Black, R., Chau, K., Moslehi, B., Cutkosky, M., editors. Exoskeletal Force-Sensing End-Effectors With Embedded Optical Fiber-Bragg-Grating Sensors; vol. 6. 2009.

[7] Kelb, C., Reithmeier, E., Roth, B.. Foil-integrated 2d optical strain sensors. Procedia Technology 2014;15:710–715. doi:10.1016/j.protcy.2014.09.042.

[8] Doany, F.E., Schow, C.L., Lee, B.G., A. Budd, R., W. Baks, C., K. Tsang, C., et al. Terabit/s-class optical pcb links incorporating 360-gb/s bidirectional 850 nm parallel optical transceivers. Journal of Lightwave Technology 2012;30(4):560–571. doi:10.1109/JLT.2011.2177244.

[9] Dingeldein, J.C., Walczak, K.A., Swatowski, B.W., Friedrich, C.R., Middlebrook, C.T., Roggemann, M.C.. Process characterization for direct dispense fabrication of polymer optical multi-mode waveguides. Journal of Micromechanics and Microengineering 2013;23(7):75015. doi:10.1088/0960-1317/23/7/075015.

[10] Bechir Hachicha, M., Kuklik, J., Overmeyer, L.. Simulation of coupling efficiency for surface integration of optical waveguides. In: 2015 6th International Conference on Modeling, Simulation, and Applied Optimization (ICMSAO). 2015, p. 1–7. doi:10.1109/ICMSAO.2015.7152259.

[11] Habenicht, G.. Kleben: Grundlagen, Technologien, Anwendungen. VDI-Buch; 6., aktualisierte aufl. ed.; Berlin, Heidelberg: Springer Berlin Heidelberg; 2009. ISBN 978-3-540-85264-3. URL: http://dx.doi.org/10.1007/978-3-540-85266-7. doi:10.1007/978-3-540-85266-7.

[12] Hachicha, B., Overmeyer, L., editors. Functionalization of UV-curing adhesives for Functionalization of UV-curing adhesives for surface-integrated micro-polymer optical fibers. SPIE Proceedings; SPIE; 2016.

[13] Denkena, B., Litwinski, K.M., Boujnah, H.. Detection of tool deflection in milling by a sensory axis slide for machine tools. Mechatronics 2015;doi:10.1016/j.mechatronics.2015.09.008.

[14] Kleppmann, W.. Taschenbuch Versuchsplanung: Produkte und Prozesse optimieren. Praxisreihe Qualitätswissen; 7., aktualisierte und erw. aufl., [elektronische ressource] ed.; München: Hanser; 2011. ISBN 978-3-446-42774-7. URL: http://www.hanser-elibrary.com/isbn/9783446427747. doi:10.3139/9783446429420.

[15] Daum, W., Krauser, J., Zamzow, P.E., Ziemann, O.. POF - Polymer Optical Fibers for Data Communication. Berlin, Heidelberg, s.l.: Springer Berlin Heidelberg; 2002. ISBN 978-3-662-04861-0. URL: http://dx.doi.org/10.1007/978-3-662-04861-0. doi:10.1007/978-3-662-04861-0.